

# Real-Time BODIPY-Binding Assay To Screen Inhibitors of the Early Oligomerization Process of A $\beta$ 1–42 Peptide

Nicolo Tonalì,<sup>\*[a, b]</sup> Veronica I. Doderò,<sup>[a]</sup> Julia Kaffy,<sup>[b]</sup> Loreen Hericks,<sup>[a]</sup> Sandrine Ongeri,<sup>[b]</sup> and Norbert Sewald<sup>\*[a]</sup>

Misfolding and aggregation of amyloid  $\beta$ 1–42 peptide (A $\beta$ 1–42) play a central role in the pathogenesis of Alzheimer's disease (AD). Targeting the highly cytotoxic oligomeric species formed during the early stages of the aggregation process represents a promising therapeutic strategy to reduce the toxicity associated with A $\beta$ 1–42. Currently, the thioflavin T (ThT) assay is the only established spectrofluorometric method to screen aggregation inhibitors. The success of the ThT assay is that it can detect A $\beta$ 1–42 aggregates with high  $\beta$ -sheet content, such as protofibrils or fibrils, which appear in the late aggregation steps. Unfortunately, by using the ThT assay, the detection of inhibitors of early soluble oligomers that present a low  $\beta$ -sheet character is challenging. Herein, a new, facile, and robust boron-dipyrromethene (BODIPY) real-time assay suitable for 96-well plate format, which allows screening of compounds as selective inhibitors of the formation of A $\beta$ 1–42 oligomers, is reported. These inhibitors decrease the cellular toxicity of A $\beta$ 1–42, although they fail in the ThT assay. The findings have been confirmed and validated by structural analysis and cell viability assays under comparable experimental conditions. It is demonstrated that the BODIPY assay is a convenient method to screen and discover new candidate compounds that slow down or stop the pathological early oligomerization process and are active in the cellular assay. Therefore, it is a suitable complementary screening method of the current ThT assay.


Alzheimer's disease (AD) is a devastating neurodegenerative disease that leads to progressive cognitive decline, functional impairment, and loss of independence.<sup>[1]</sup> The number of people worldwide suffering from AD is expected to reach 75 million by 2030,<sup>[2]</sup> but no causative treatment exists for AD.


The search for small molecules that inhibit the aggregation of the 42-residue amyloid  $\beta$  protein fragment (A $\beta$ 1–42; Figure 1 A) is still ongoing to find a therapy for AD. A $\beta$ 1–42 spontaneously self-associates into soluble oligomers and insoluble aggregates, such as protofibrils and fibrils with high  $\beta$ -sheet content. It has been recognized that small and soluble A $\beta$ 1–42 oligomers are particularly cytotoxic.<sup>[3–7]</sup> Thus, therapeutic strategies that intervene in the early oligomerization process, rather than in the later fibril formation step, have recently attracted attention.<sup>[8]</sup> However, despite its therapeutic significance, the screening of potential inhibitors of the early oligomerization process is still challenging. The thioflavin T (ThT) fluorescence assay is used routinely to determine the influence of compounds on amyloid aggregation kinetics.<sup>[9,10]</sup> However, ThT only exhibits a substantial fluorescence increase upon binding to  $\beta$ -sheet-rich amyloid protofilaments and fibrils, but has low sensitivity to soluble early-stage oligomers.<sup>[11–14]</sup> Molecules that do not show any apparent inhibition of amyloid aggregation, according to the ThT assay, are usually not considered for any subsequent testing. It may be presumed that several lead compounds have been discarded, although they would be capable of preventing the formation of small cytotoxic oligomers. Conversely, a variety of compounds that were effective inhibitors in the ThT assay might have been evaluated for further preclinical trials, but later were discontinued because they interfered with fibril formation, but were ineffective at preventing the formation of cytotoxic oligomeric species.<sup>[15]</sup> Consequently, the improvement of fluorescent probes to specifically detect oligomers is highly relevant and, in particular, the development of new screening assays specific for the early oligomerization process is of high current interest.<sup>[16–20]</sup>

Herein, we report the development of a new real-time 96-well plate assay based on a BODIPY dye that is applicable to screen and discover new inhibitors of early A $\beta$ 1–42 oligomerization, which fail to be discovered in the typical ThT assay. The employed BODIPY dye, containing a triazole moiety (Figure 1 A), is a suitable probe for protein hydrophobicity and amyloid conformational transitions, even at a low dye concentration (0.53  $\mu$ M).<sup>[16]</sup> The BODIPY real-time 96-well plate assay combines high sensitivity towards A $\beta$ 1–42 soluble oligomers and statistical robustness of the kinetics curve obtained under oligomerization conditions. By testing five designed inhibitors, we were able to prove that the inhibitory activity detected by the BODIPY assay perfectly correlated with reduced A $\beta$ 1–42 toxicity on neuroblastoma cells. Furthermore, functional information provided by the novel BODIPY assay could be correlated with structural information of the inhibition process.

[a] Dr. N. Tonalì, Dr. V. I. Doderò, L. Hericks, Prof. Dr. N. Sewald  
Organic and Bioorganic Chemistry  
Department of Chemistry, Bielefeld University  
P.O. Box 100131, 33501 Bielefeld (Germany)  
E-mail: norbert.sewald@uni-bielefeld.de

[b] Dr. N. Tonalì, Dr. J. Kaffy, Prof. Dr. S. Ongeri  
BioCIS, CNRS/Université Paris Sud, Université Paris Saclay  
5 rue Jean-Baptiste Clément, 92296 Châtenay-Malabry Cedex (France)  
E-mail: nicolo.tonali@u-psud.fr

 Supporting information and the ORCID identification numbers for the authors of this article can be found under <https://doi.org/10.1002/cbic.201900652>.

 © 2019 The Authors. Published by Wiley-VCH Verlag GmbH & Co. KGaA. This is an open access article under the terms of the Creative Commons Attribution Non-Commercial NoDerivs License, which permits use and distribution in any medium, provided the original work is properly cited, the use is non-commercial and no modifications or adaptations are made.

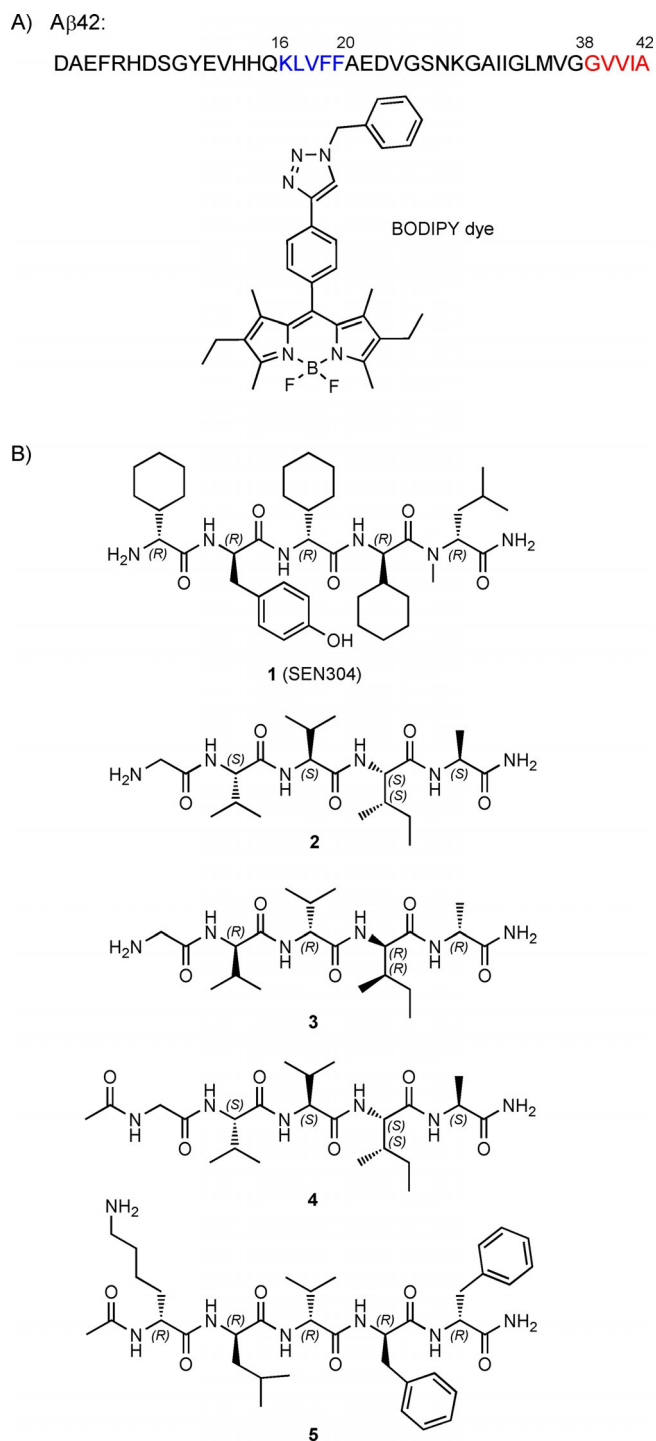


**Figure 1.** A) Primary sequence of A $\beta$ 1–42 peptide: in color, the two “hot spot” aggregation fragments; chemical structure of the boron-dipyrromethene (BODIPY) dye employed in this study. B) Molecular structures of inhibitors of the A $\beta$ 1–42 aggregation process: SEN304 (**1**)<sup>[11]</sup> and the four newly designed peptides, **2–5**, employed in this study.

As a benchmark to compare BODIPY and ThT assays, we tested **1** (Figure 1B); this is an established potent inhibitor of A $\beta$  cytotoxicity able to perturb A $\beta$  oligomer and fibril formation.<sup>[21]</sup> Furthermore, four newly designed peptides, **2–5** (Figure 1B), were investigated as inhibitors of the formation of toxic A $\beta$ 1–42 oligomers by targeting the two A $\beta$ 1–42 aggrega-

tion hot spots: KLVFF and GVVIA (Figure 1A, in blue and red, respectively). Our selection was based on previous evidence that tetrapeptide derivatives of the C-terminal part of A $\beta$  (39–42) acted as suitable inhibitors of A $\beta$ -induced toxicity, but were poor inhibitors of fibril formation.<sup>[22–24]</sup> Three new pentapeptide analogues of A $\beta$  (38–42) were synthesized (**2–4**) to study whether the elongation of the sequence and/or the stereochemistry of the amino acids could influence the inhibitory activity. A glycine residue was additionally introduced to impart flexibility and to generate an anchor site for conjugation. Furthermore, the peptide A $\beta$  (16–20), which corresponds to the hydrophobic central region of A $\beta$ , plays an essential role in A $\beta$ –A $\beta$  interactions because it binds to  $\beta$  sheets and nucleates aggregation.<sup>[25–28]</sup> Therefore, the all-D-configured acetylated analogue, **5**,<sup>[29]</sup> was also tested.

In general, reproducibility is difficult to achieve when measuring and characterizing protein aggregation kinetics, mainly due to the existence of different species whose composition highly depends on the experimental handling of amyloid peptides.<sup>[30,31]</sup>

The ThT assay of A $\beta$ 1–42 routinely requires fast aggregation conditions mainly allowing for the detection of fibrils, named here as Protocol A (see the Supporting Information for experimental details).<sup>[14]</sup> Under the same conditions, BODIPY detects both soluble oligomers and protofibrils (Figure 2A and Figure S1A in the Supporting Information). BODIPY fluorescence intensity already increases from the beginning of the kinetics, whereas the ThT fluorescence is maintained stably low up to 8 h (known as lag phase). As shown previously,<sup>[32–34]</sup> under fast aggregation conditions, reproducibility is still a challenge; this is directly related to the difficulty of having A $\beta$ 1–42 in a monomeric form at the beginning of the aggregation, the formation of different species with different binding affinities for the dye, and the precipitation of insoluble fibrils.<sup>[31]</sup>

In this context, a reconstitution protocol of A $\beta$ 1–42 that slows down the aggregation kinetics was developed, which is referred to herein as Protocol B (see the Supporting Information for experimental details). Under these slow aggregation conditions, time-dependent A $\beta$ 1–42 oligomerization was followed by BODIPY or ThT dye in a 96-well plate setup and compared. As expected, in the absence of fibrils, ThT fluorescence remained low during this experimental phase (Figures 2B and S1B, blue curve). Although both dyes showed an exponential kinetic curve, the increase in the fluorescence in the case of ThT was considerably lower than that of BODIPY (Figures 2B and S1B, red curve). Thus, by using only the ThT assay, it is challenging to compare between weak and potent inhibitors of oligomerization. The small increase in the signal could be associated to the fact that ThT fails to detect all types of oligomers, especially those with low amounts of  $\beta$  sheets, as described recently by Sang et al.<sup>[12]</sup> On the other hand, the fluorescence intensity of BODIPY (Figures 2B and S1B, red curve) showed a pronounced exponential kinetic curve, as characterized by an elongation slope between 0 and 4 h and a steady state between 5 and 15 h (Figures 2B and S1B), followed by a slight increase at 24 h (Figure S1C). The higher detection sensitivity of BODIPY is correlated not only to its higher receptive-

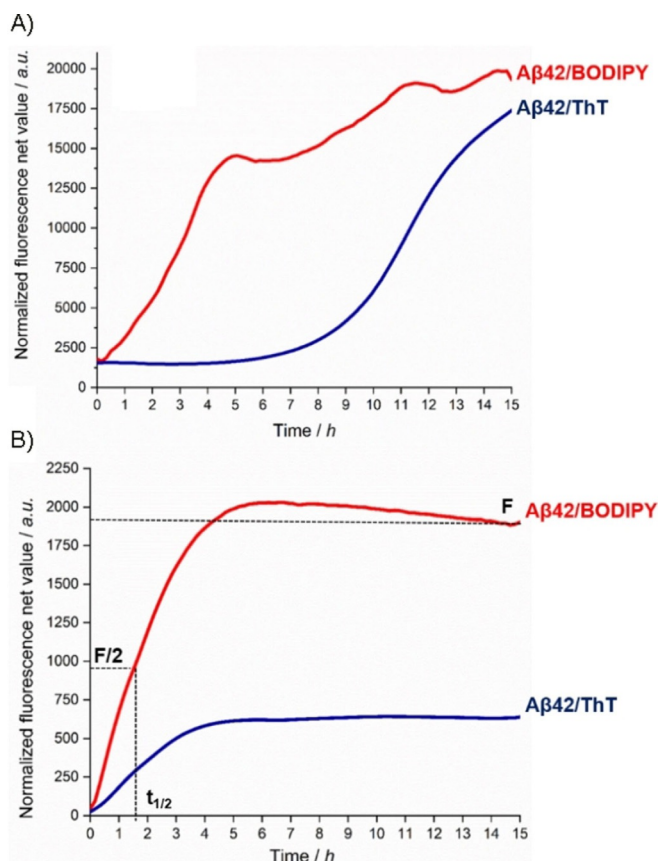


**Figure 2.** A comparison of BODIPY (red) and ThT (blue) fluorescence intensity over time in 96-well plate format in the presence of Aβ1–42 (10 μM) during either A) fibril formation (Protocol A) or B) oligomerization (Protocol B). The data are presented as normalized fluorescence net values. The curves represent the average of measurements made in triplicate from two different experiments (for error bars, see Figure S1 A and B). For details, see the Supporting Information.

ness to hydrophobicity, but also to the β-sheet structure, as described previously.<sup>[16]</sup> Three parameters can be derived from the ThT and BODIPY fluorescence kinetic curves:  $t_{1/2}$ , which is defined as the time at which the fluorescence has reached 50% of its maximum (as a measure of the process rate), the slope of the elongation phase of the curve (as a measure of the process rate), and  $F$ , which is the fluorescence value of the final plateau and is assumed to depend on the number of aggregates formed.

The presence of Aβ1–42 oligomers up to 8 h was confirmed by means of TEM analysis (Figure 3A). The stability of oligomers under the oligomerization protocol was also observed by means of SDS-PAGE analysis,<sup>[21]</sup> even after heating in reducing Laemmli buffer (Figures 3B and S2). At the early time points (0 and 2 h), bands corresponding to residual tri- (≈ 13.5 kDa), tetra- (≈ 18 kDa), and pentamers (≈ 22.5 kDa) were still observed, even under denaturing conditions. At the same time, deca- (≈ 45 kDa) and dodecamers (≈ 54 kDa), which are important in the etiology of AD,<sup>[35]</sup> were fainter than that of the small, soluble oligomers, but, due to oligomerization, became slightly stronger at 4 and 8 h (Figures 3B and S2). Moreover, time-dependent CD experiments confirmed the slow transition

from unordered to ordered oligomers in the first 3 h (Figure 3C), as evident by the slow increase of the minima at  $\lambda \approx 215$  nm and the maxima at  $\lambda = 195$  nm until 7 h. An isodichroic point was observed at  $\lambda = 208$  nm, which suggested a two-state transition from random coil to β-sheet conformation (Figure 3C).<sup>[36]</sup> CD deconvolution with the algorithm BeStSel<sup>[37,38]</sup> revealed an increase in the amount of β sheets within 1 h (Figures 3D and S3). The ratio between β-sheet structure and unordered conformation increased by 84% for 5 h. The antiparallel β-sheet structure, formed in the early oligomerization phase, is the major component that tends to increase during the first hour. Successively, the decrease in the antiparallel component is compensated for by an increase in the parallel one (Figure 3D).

Based on the abovementioned results, we screened compounds 2–5 as potential inhibitors of Aβ1–42 aggregation under the optimized experimental conditions in a 96-well format (Figures 4 and S4). Protocol A, with the ThT assay, was employed to screen the inhibition of fibril formation (Figures 4A, C, and S4). On the other hand, to screen oligomerization inhibitors, Protocol B and the BODIPY dye were used (Figures 4B, D, and S5–S9). Each compound was tested at tenfold excess (100 μM) and at a 1:1 ratio (10 μM). For both experiments, the three valuable parameters ( $t_{1/2}$ , the slope of the curve, and  $F$ ) for high-throughput screening were obtained from the fluorescence curves and are compiled in Table 1. In Figure 4, we present the two time-course fluorescence experiments for compounds 1 and 2 with either ThT or BODIPY. As expected, positive control 1 was active at both 10:1 and 1:1 ratios under both experimental conditions (Figures 4A, B, S4, and S5A). For screening with the ThT assay (Protocol A), no significant activity was observed for the C-terminal analogues 2 (Figure 4C and Table 1) and 4 at both ratios (Figure S4), whereas a slight delay of the aggregation in a concentration-dependent manner was shown for the all-D-configured peptide 3 kinetic curve (Figure S4). Compound 5 proved to be a full inhibitor of fibril formation at a 10:1 ratio, whereas only a slight delay of the kinetics was observed at a 1:1 ratio (Figure S4). According to the ThT assay, the C-terminal fragments (2, 3, and 4) are not inhibitors, whereas compounds 1 and 5 are efficient inhibitors of the fibril formation process (Table 1).

On the other hand, the BODIPY fluorescence assay revealed that all designed peptides (2–5) interfered with early oligomer formation, as summarized in Table 1. Compounds 2 (Figures 4D and S5B, Table 1) and 4 (Figure S6) are both able to significantly reduce the BODIPY slope and fluorescence at 10:1 ratio, which indicates an inhibitory effect on the early oligomerization process. Importantly, only non-acetylated analogue 2 still showed a substantial reduction of the fluorescence intensity at 1:1 ratio (Figures 4D and S5B). An additional experiment showed that the full inhibitory activity of 2 on the oligomerization process was maintained at a 5:1 ratio (Figure S7). Peptide 3, which is the mirror image of 2, also suppressed oligomer formation at a 10:1 ratio, but at a 1:1 ratio only a slight inhibitory effect was observed (Figure S8). Non-acetylated derivative 2 was more effective than that of its mirror image, 3, and its acetylated analogue, 4. This differs from the ThT test, in



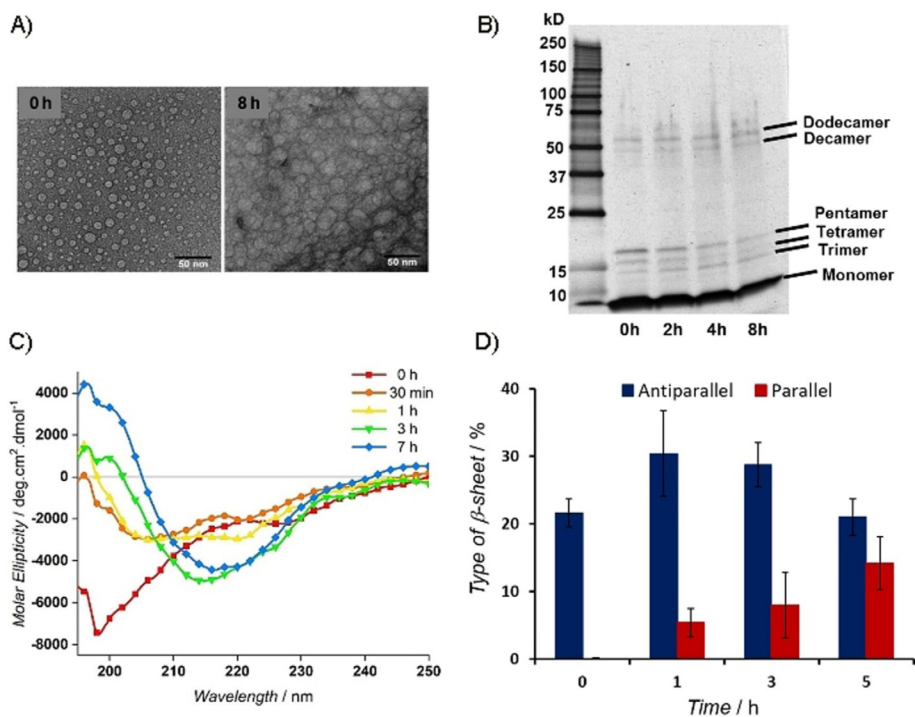


**Figure 3.** Time course of Aβ1-42 (10 μM) oligomerization in 20 mM phosphate-buffered saline (PBS) at pH 7.4 (Protocol B). A) TEM images of Aβ1-42 at initial and final time points (8 h). B) SDS-PAGE results showing the presence of monomeric and different small oligomeric species of Aβ1-42. C) Secondary structure of Aβ1-42 (25 μM) monitored by means of circular dichroism (CD). D) Estimated type of β-sheet structure content, by deconvolution of CD results with the algorithm BeStSel.

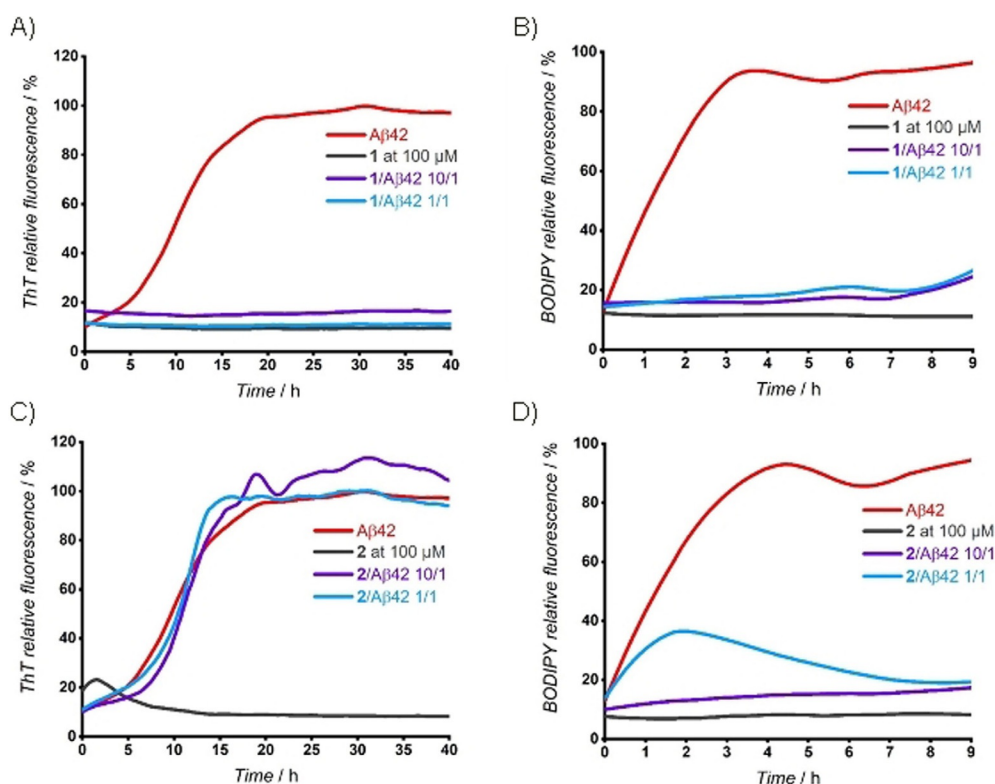


**Figure 4.** Time-course fluorescence experiments with ThT (A and C; Protocol A: fibril formation) and BODIPY (B and D; Protocol B: oligomerization). Aβ1-42 (10 μM) without inhibitors (red) and in the presence of compounds 1 or 2 at compound/Aβ42 ratios of 10:1 (purple curve) and 1:1 (light blue curve). In all experiments, the interactions of 1 or 2 with the fluorescent dyes in the absence of Aβ42 are represented by a gray line. For experimental details and statistical analysis, see the Supporting Information.

**Table 1.** Effects of compounds 1–5 on 10  $\mu\text{M}$  A $\beta$ 42 fibril formation and oligomerization, as assessed by ThT- and BODIPY-fluorescence spectroscopy, respectively. Compounds were tested at compound/A $\beta$ 42 ratios of 10:1 and 1:1 and compared with the values obtained for A $\beta$ 1–42 alone ( $t_{1/2}$ ,  $F$ , and slope).

Fibril formation: Protocol A			Oligomerization: Protocol B			
Compound (compound/A $\beta$ ratio)	$t_{1/2}$ extension/reduction <sup>[a]</sup>	$F$ reduction [%] <sup>[b]</sup>	Compound (compound/A $\beta$ ratio)	$t_{1/2}$ extension/reduction <sup>[a]</sup>	$F$ reduction [%] <sup>[b]</sup>	Slope reduction [%] <sup>[c]</sup>
1 (10:1)	n.a. <sup>[c]</sup>	$-85 \pm 2$	1 (10:1)	n.a.	$-75$	$-99$
1 (1:1)	n.a.	$-89 \pm 2$	1 (1:1)	n.a.	$-73$	$-95$
2 (10:1)	n.e. <sup>[d]</sup>	n.e.	2 (10:1)	n.a. <sup>[d]</sup>	$-81$	$-94$
2 (1:1)	n.e.	n.e.	2 (5:1)	n.a. <sup>[d]</sup>	$-82$	$-100$
3 (10:1)	$+77 \pm 15$	n.e.	2 (1:1)	r.a. <sup>[e]</sup> (from 110 min)	$-80$	$-9$ (110 min)
3 (1:1)	$+39 \pm 36$	n.e.	3 (10:1)	n.a.	$-78$	$-91$
4 (10:1)	$-16 \pm 8$	$-14 \pm 4$	3 (1:1)	r.a. (from 120 min)	$-47$	$+8$
4 (1:1)	$-15 \pm 10$	$-15 \pm 5$	4 (10:1)	n.a.	$-78$	$-95$
5 (10:1)	n.a.	$-85 \pm 2$	4 (1:1)	n.e.	$-8$	$-15$
5 (1:1)	$+154 \pm 23$	n.e.	5 (10:1)	n.a.	$-86$	$-93$
			5 (1:1)	n.a.	$-84$	$-94$

See the Supporting Information for details of the calculation of [a]  $t_{1/2}$  extension, [b]  $F$  reduction, and [c] slope reduction. [d] n.a.: no aggregation. [e] r.a.: reduction of aggregation. [f] n.e.: no effect. Parameters are calculated from the mean curves, as derived by statistical analysis of data after triplicate measurements for each condition and at least two independent experiments.

which compound **3** was more active than that of the other two. In summary, these results provide strong evidence that the C-terminal fragments (**2**, **3**, and **4**) can inhibit and disrupt the early oligomerization process of A $\beta$ 1–42, but are not adequate at reducing late fibril formation. A promising effect was also observed for pentapeptide **5**, which was revealed to be a very potent inhibitor of the oligomerization process and of the fibril formation. Compound **5** was able to almost fully suppress BODIPY fluorescence intensity, and thus, to dramatically decrease early oligomerization at both 10:1 and 1:1 ratios (Figure S9).

To validate the screening results obtained by the BODIPY assay, we tested the effective rescue of SH-SY5Y neuroblastoma cells by using lead compounds **2**, **4**, and **5** in a 3-(4,5-dimethylthiazol-2-yl)-5-(3-carboxymethoxyphenyl)-2-(4-sulfophenyl)-2H-tetrazolium (MTS) viability assay (Figure 5). Positive controls **1** and resveratrol were included because of their known ability to rescue neuroblastoma cells from cytotoxic A $\beta$ 1–42. The addition of compound **2** showed a protective effect on the cells from cytotoxic A $\beta$ 1–42 oligomers at both 5:1 and 1:1 ratios (2/A $\beta$ 1–42). The N-acetylated compound, **4**, was active only at a 5:1 ratio, but the protective effect was lost at 1:1 ratio; this indicated that **4** was less efficient than that of **2** at reducing A $\beta$ 1–42 toxicity. This result is in accordance with the BODIPY assay, which shows the superiority of **2** over **4** at reducing the formation of toxic early oligomers. Neither compound, if incubated alone with cells at high concentration, showed any toxicity. The activity of **2** was very similar to that observed for compounds **1** and **5**, which were inhibitors of both oligomerization and fibril formation (Figure 4). This demonstrates that the BODIPY assay is a valuable method for screening compounds that are either specific inhibitors of the oligomerization process or mixed inhibitors of both processes. Compound **1** was toxic itself to the SH-SY5Y neuroblastoma cells, although this was not observed if A $\beta$  was present, which suggested that its toxicity decreased upon interaction with A $\beta$ 1–42. On the contrary, compounds **2** and **5** did not show any toxicity if incu-

bated alone with cells. The protective effect of **2** was also comparable to that of resveratrol, which currently is in clinical trials.<sup>[39,40]</sup>

Finally, the behavior of lead compound **2** during the early stages of A $\beta$ 1–42 oligomerization was further investigated by means of SDS-PAGE and CD spectroscopy analyses. In the SDS-PAGE experiment, at a 5:1 ratio (compound **2**/A $\beta$ 1–42), a change of the residual A $\beta$ 1–42 oligomer distribution was observed. It seems that **2** can reduce the formation of early oligomers, such as tri-, tetra-, and pentamers, but promotes the formation of species with a high molecular weight that, according

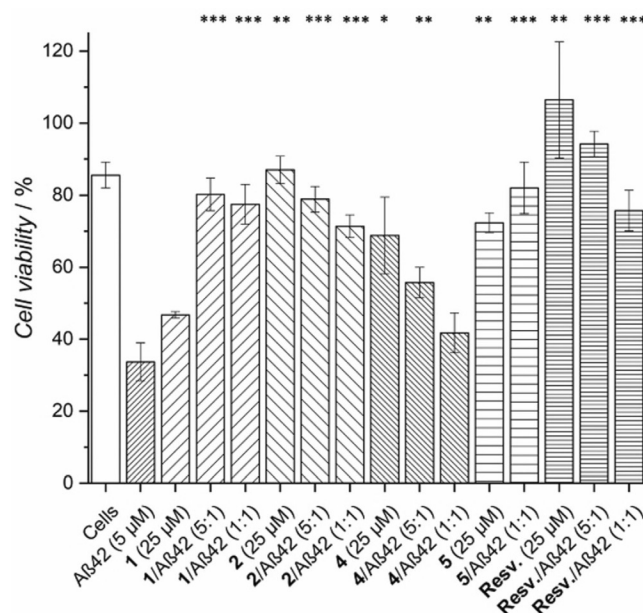


**Figure 5.** Cell viability assay results, representing the percentage of survival observed for cells incubated without A $\beta$ 42, with only inhibitors, and with 5  $\mu\text{M}$  A $\beta$ 1–42 with or without the different inhibitors. A statistically significant difference between A $\beta$ 42-treated cells with and without inhibitor is indicated by \* $p < 0.05$ , \*\* $p < 0.01$ , and \*\*\* $p < 0.001$ ;  $n = 6$  for each condition.

to cell viability experiments, are not toxic to the cell ( $t=0$ ; Figure 6A). The change in the oligomerization pathway, compared to that of A $\beta$ 1–42 alone (Figure 3B), might be responsible for the reduction of A $\beta$ 1–42 toxicity. CD spectroscopy of A $\beta$ 1–42

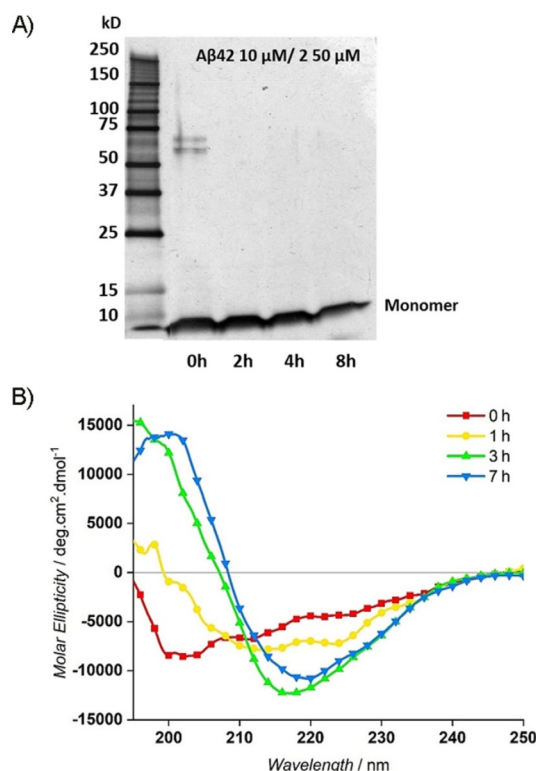


**Figure 6.** The A $\beta$ 42 oligomerization pathway in the presence of compound **2** in 20 mM PBS buffer at pH 7.4. A) SDS-PAGE and silver-stained glycine gel, showing the A $\beta$ 42 (10  $\mu$ M) oligomeric species at 0, 2, 4, and 8 h in the presence of 50  $\mu$ M **2** (2/A $\beta$ 42, 5:1); B) CD time-dependent experiment of A $\beta$ 42 (20  $\mu$ M) in the presence of 100  $\mu$ M **2** (2/A $\beta$ 42, 5:1). Deconvolution was performed on the results of CD measurements, after subtraction of the corresponding buffer or the solution containing a 5:1 concentration of inhibitor.

in the presence of **2** (Figure 6B) indicates that **2** considerably increases the ordered state of A $\beta$ 1–42 from the early stages by increasing, in particular, the  $\beta$ -sheet percentage (Figure S11). This suggests that a subtle change in A $\beta$ 1–42 conformation may reduce its toxicity, as shown in the cellular experiments. Further experiments will be performed to understand the exact mechanism of inhibition.<sup>[41]</sup>

In conclusion, the real-time BODIPY assay is an efficient method to monitor the early stages of A $\beta$ 1–42 peptide oligomerization and to evaluate in vitro small peptide inhibitors of the toxic A $\beta$ 1–42 oligomerization pathway. In this regard, the BODIPY assay proved suitable for the discovery of new, active inhibitors of early oligomerization of A $\beta$ 1–42, such as compound **2**, which did not interfere with the fibril formation process, and thus, was missed in the routine ThT screening assay. Importantly, the real-time BODIPY-binding 96-well assay is suitable for the routine screening of larger compound libraries because of the reproducibility and statistical robustness, as demonstrated herein. Finally, our findings reveal that both screening methods are complementary to allow a more efficient

screening of inhibitors that actively interfere in A $\beta$ 1–42 fibril formation and/or oligomerization and are active in the subsequent cellular assay. Therefore, the implementation of the real-time BODIPY assay may facilitate the discovery of lead compounds that can selectively inhibit the early oligomerization of A $\beta$ 1–42.

## Acknowledgements

We acknowledge Dr. Yvonne Hannappel for the acquisition of TEM images and Dr. Sarah Bregant for fruitful discussions.

## Conflict of Interest

The authors declare no conflict of interest.

**Keywords:** Alzheimer's disease · amyloid beta-peptides · fluorescence · inhibitors · oligomerization

- [1] F. Panza, V. Solfrizzi, B. P. Imbimbo, R. Tortelli, A. Santamato, G. Logroscino, *Rev. Clin. Immunol.* **2014**, *10*, 405–419.
- [2] M. Prince, A. Comas-Herrera, M. Knapp, M. Guerchet, M. Karagiannidou, *World Alzheimer Report 2016*, Alzheimer's Disease International, London, **2016**, <https://www.alz.co.uk/research/WorldAlzheimerReport2016.pdf>.
- [3] D. B. Teplow, *Alzheimers Res. Ther.* **2013**, *5*, 39–50.
- [4] D. B. Teplow, N. D. Lazo, G. Bitan, S. Bernstein, T. Wyttentbach, M. T. Bowers, A. Baumketner, J. E. Shea, B. Urbanc, L. Cruz, J. Borreguero, H. E. Stanley, *Acc. Chem. Res.* **2006**, *39*, 635–645.
- [5] P. Prangko, E. C. Yusko, D. Sept, J. Yang, M. Mayer, *PLoS One* **2012**, *7*, e47261.
- [6] P. Cizas, R. Budvytyte, R. Morkuniene, R. Moldovan, M. Broccio, M. Lösche, G. Niaura, G. Valincius, V. Borutaite, *Arch. Biochem. Biophys.* **2010**, *496*, 84–92.
- [7] I. Benilova, E. Karran, B. De Strooper, *Nat. Neurosci.* **2012**, *15*, 349–357.
- [8] E. McDade, R. J. Bateman, *Nature* **2017**, *547*, 153–155.
- [9] M. R. Nilsson, *Methods* **2004**, *34*, 151–160.
- [10] M. Biancalana, S. Koide, *Biochim. Biophys. Acta Proteins Proteomics* **2010**, *1804*, 1405–1412.
- [11] A. Hawe, M. Sutter, W. Jiskoot, *Pharm. Res.* **2008**, *25*, 1487–1499.
- [12] J. C. Sang, J.-E. Lee, A. J. Dear, S. De, G. Meisl, A. M. Thackray, R. Bujdoso, T. P. J. Knowles, D. Klenerman, *Chem. Sci.* **2019**, *10*, 4588–4597.
- [13] B. Morel, M. P. Carrasco, S. Jurado, C. Marcob, F. Conejero-Lara, *Phys. Chem. Chem. Phys.* **2018**, *20*, 20597–20614.
- [14] N. D. Younan, J. H. Viles, *Biochemistry* **2015**, *54*, 4297–4306.
- [15] L. P. Jameson, N. W. Smith, S. V. Dzyuba, *ACS Chem. Neurosci.* **2012**, *3*, 807–819.
- [16] N. W. Smith, A. Alonso, C. M. Brown, S. V. Dzyuba, *Biochem. Biophys. Res. Commun.* **2010**, *391*, 1455–1458.
- [17] L. P. Jameson, S. V. Dzyuba, *Bioorg. Med. Chem. Lett.* **2013**, *23*, 1732–1735.
- [18] P. Hammarström, R. Simon, S. Nyström, P. Konradsson, A. Aslund, K. P. Nilsson, *Biochemistry* **2010**, *49*, 6838–6845.
- [19] C. L. Teoh, D. Su, S. Sahu, S. W. Yun, E. Drummond, F. Prelli, S. Lim, S. Cho, S. Ham, T. Wisniewski, Y. T. Chang, *J. Am. Chem. Soc.* **2015**, *137*, 13503–13509.
- [20] J. Hatai, L. Motiei, D. Margulies, *J. Am. Chem. Soc.* **2017**, *139*, 2136–2139.
- [21] H. Amijee, C. Bate, A. Williams, J. Virdee, R. Jeggo, D. Spanswick, D. I. C. Scopes, J. M. Treherne, S. Mazzitelli, R. Chawner, C. E. Eyers, A. J. Doig, *Biochemistry* **2012**, *51*, 8338–8352.
- [22] X. Zheng, C. Wu, D. Liu, H. Li, G. Bitan, J.-E. Shea, M. T. Bowers, *J. Phys. Chem. B* **2016**, *120*, 1615–1623.
- [23] M. M. Gessel, C. Wu, H. Li, G. Bitan, J.-E. Shea, M. T. Bowers, *Biochemistry* **2012**, *51*, 108–117.

- [24] H. Li, Z. Du, D. H. J. Lopes, E. A. Fradinger, C. Wang, G. Bitan, *J. Med. Chem.* **2011**, *54*, 8451–8460.
- [25] C. Soto, E. M. Siquerdsson, L. Morelli, R. A. Kumar, E. M. Castaño, B. Frangione, *Nat. Med.* **1998**, *4*, 822–826.
- [26] C. Soto, M. S. Kindy, M. Baumann, B. Frangione, *Biochem. Biophys. Res. Commun.* **1996**, *226*, 672–680.
- [27] T. Takahashi, H. Mihara, *Acc. Chem. Res.* **2008**, *41*, 1309–1318.
- [28] B. Neddenriep, A. Calciano, D. Conti, E. Sauve, M. Paterson, E. Bruno, D. A. Moffet, *Open Biotechnol. J.* **2011**, *5*, 39–46.
- [29] T. Arai, T. Araya, D. Sasaki, A. Taniguchi, T. Sato, Y. Sohma, M. Kanai, *Angew. Chem. Int. Ed.* **2014**, *53*, 8236–8239; *Angew. Chem.* **2014**, *126*, 8375–8378.
- [30] N. Benseny-Cases, O. Klementiera, J. Clesdera, *Subcell. Biochem.* **2012**, *65*, 53–74.
- [31] L. Giehm, D. E. Otzen, *Anal. Biochem.* **2010**, *400*, 270–281.
- [32] S. Pellegrino, N. Tonali, E. Erba, J. Kaffy, M. Taverna, A. Contini, M. Taylor, D. Allsop, M. Taverna, S. Ongerì, *Chem. Sci.* **2017**, *8*, 1295–1302.
- [33] J. Kaffy, D. Brinet, J.-L. Soulier, I. Correia, N. Tonali, K. F. Fera, Y. Iacone, A. R. F. Hoffmann, L. Khemtémourian, B. Crousse, M. Taylor, D. Allsop, M. Taverna, O. Lequin, S. Ongerì, *J. Med. Chem.* **2016**, *59*, 2025–2040.
- [34] N. Tonali, J. Kaffy, J.-L. Soulier, M. L. Gelmi, E. Erba, M. Taverna, C. van Heijenoort, T. Ha-Duong, S. Ongerì, *Eur. J. Med. Chem.* **2018**, *154*, 280–293.
- [35] S. L. Bernstein, N. F. Dupuis, N. D. Lazo, T. Wyttenbach, M. M. Condron, G. Bitan, D. B. Teplow, J. E. Shea, B. T. Ruotolo, C. V. Robinson, M. T. Bowers, *Nat. Chem.* **2009**, *1*, 326–331.
- [36] M. G. Herrera, F. Zamarreno, M. Costabel, H. Ritacco, A. Hütten, N. Sewald, V. I. Doderó, *Biopolymers* **2014**, *101*, 96–106.
- [37] A. Micsonai, F. Wien, L. Kernya, Y.-H. Lee, Y. Goto, M. Réfrégiers, J. Kardos, *Proc. Natl. Acad. Sci. USA* **2015**, *112*, E3095–E3103.
- [38] P. Misra, R. Kodali, S. Chemuru, K. Kar, R. Wetzel, *Nat. Commun.* **2016**, *7*, 12419.
- [39] Y. Feng, X.-P. Wang, S. G. Yang, Y. J. Wang, X. Zhang, X. T. Du, X. X. Sun, M. Zhao, L. Huang, R. T. Liu, *NeuroToxicology* **2009**, *30*, 986–995.
- [40] A. R. A. Ladiwala, J. C. Lin, S. S. Bale, A. M. Marcelino-Cruz, M. Bhattacharya, J. S. Dordick, P. M. Tessier, *J. Biol. Chem.* **2010**, *285*, 24228–24237.
- [41] S. Chia, J. Habchi, T. C. T. Michaels, S. I. A. Cohen, S. Linse, C. M. Dobson, T. P. J. Knowles, M. Vendruscolo, *Proc. Natl. Acad. Sci. USA* **2018**, *115*, 10245–10250.

---

Manuscript received: October 28, 2019

Accepted manuscript online: November 8, 2019

Version of record online: January 9, 2020